



RESEARCH ARTICLE

Disfavoring Macrocycle b Fragments by Constraining Torsional Freedom: The “Twisted” Case of QWFGLM b₆

Marcus Tirado,¹ Jochem Rutters,² Xian Chen,^{1,4} Alfred Yeung,¹ Jan van Maarseveen,² John R. Eyler,¹ Giel Berden,³ Jos Oomens,^{2,3} Nick C. Polfer¹

¹Department of Chemistry, University of Florida, P.O. Box 117200, Gainesville, FL 32611-7200, USA

²Van't Hoff Institute for Molecular Sciences, University of Amsterdam, Science Park 904, 1098 XH, Amsterdam, The Netherlands

³FOM Institute for Plasma Physics Rijnhuizen, Edisonbaan 14, 3439 MN, Nieuwegein, The Netherlands

⁴Now at Department of Chemistry, University of Illinois, Urbana, IL 61801, USA

Abstract

While recent studies have shown that for some peptides, such as oligoglycines and Leu-enkephalin, mid-sized b fragment ions exist as a mixture of oxazolone and macrocycle structures, other primary structure motifs, such as QWFGLM, are shown to exclusively give rise to macrocycle structures. The aim of this study was to determine if certain amino acid residues are capable of suppressing macrocycle formation in the corresponding b fragment. The residues proline and 4-aminomethylbenzoic acid (**4AMBz**) were chosen because of their intrinsic rigidity, in the expectation that limited torsional flexibility may impede “head-to-tail” macrocycle formation. The presence of oxazolone versus macrocycle b₆ fragment structures was validated by infrared multiple photon dissociation (IRMPD) spectroscopy, using the free electron laser FELIX. It is confirmed that proline disfavors macrocycle formation in the cases of QPWFGLM b₇ and in QPFGLM b₆. The **4AMBz** substitution experiments show that merely QWFG(**4AMBz**)M b₆, with **4AMBz** in the fifth position, exhibits a weak oxazolone band. This effect is likely ascribed to a stabilization of the oxazolone structure, due to an extended oxazolone ring-phenyl π-electron system, not due to the rigidity of the **4AMBz** residue. These results show that some primary structures have an intrinsic propensity to form macrocycle structures, which is difficult to disrupt, even using residues with limited torsional flexibility.

Key words: IR spectroscopy, SORI CID, H/D exchange, Cyclization, Oxazolone, Macrocycle, Peptide rearrangement, Proline, 4-Aminomethylbenzoic acid

Introduction

The underlying chemistry of collision-induced dissociation (CID) of protonated peptides is governed by

nucleophilic attacks. The amide bond is the most labile backbone bond in peptides under low-energy CID conditions. Cleavage of the amide bond is mediated by a nucleophilic attack from an adjacent backbone carbonyl, giving rise to “b” fragments with a C-terminal oxazolone ring. The presence of this five-membered ring is consistent with the stability of b fragments [1, 2], as opposed to labile linear acylium structures. Nonetheless, it was found that oxazolone structures can undergo a complex rearrangement, involving a nucleophilic attack from the N-terminus, and

Electronic supplementary material The online version of this article (doi:10.1007/s13361-011-0315-5) contains supplementary material, which is available to authorized users.

Correspondence to: Nick C. Polfer; e-mail: polfer@chem.ufl.edu

resulting in “head-to-tail” macrocycle structures. The occurrence of macrocycle structures is a central tenet to the scrambling hypothesis by Paizs and coworkers [3], as the macrocycle may not always reopen where it was originally formed. Subsequent fragmentation from these permuted sequences leads to non-direct/permuted/scrambled CID product ions in tandem mass spectra. The appearance of such permuted sequence ions has been verified for select peptide systems [4–8], as well as for tandem mass spectra from proteomics data [9–11].

A deeper comprehension of the fragmentation chemistry in CID can be obtained by employing structural techniques that confirm the ion structures and mechanistic pathways for biomolecules in the gas phase. Gas-phase hydrogen/deuterium exchange (HDX) [12], infrared multiple photon dissociation (IRMPD) spectroscopy [13, 14], and ion mobility mass spectrometry [15–17] have all been applied to this task.

Gas-phase hydrogen/deuterium exchange (HDX) measures the reaction rate of the CID product with a deuterating agent (e.g., CH₃OD, ND₃) [12]. “Fast-” and “slow-”-exchanging b fragment structures have been distinguished in this way by a number of groups [18–23]. Quantification of “fast” versus “slow” structures can be performed by an analysis of the kinetic rates. Nonetheless, while HDX can give important insights into the make-up of structural isomers of CID product ions, the structural interpretation of HDX results is often less straightforward.

In IRMPD spectroscopy, the product ion of interest is photodissociated with a tunable infrared laser. The infrared spectrum of an ion reveals information on the chemical structure by means of diagnostic vibrational frequencies. Thus, the oxazolone structure can be confirmed via the presence of a lactone-type C=O stretch band, which appears in the high-frequency region (1770–1950 cm⁻¹) of the mid-infrared spectrum [24, 25]. Studies by several groups have shown that smaller b fragments, such as b₂, typically form oxazolone structures [18, 21, 26–28]. An exception to this rule is the b₂ sequence motif His-Ala, which mainly adopts a diketopiperazine structure [19].

For mid-sized to larger b fragments, there appears to be a higher prevalence for forming “head-to-tail” macrocycle structures. In an IR spectroscopic study by Maitre and coworkers, the b₅ fragment from (Gly)₅R was shown to exclusively give rise to macrocycle structures [29]. In a complementary IRMPD spectroscopy and HDX study on oligoglycine b fragments, Chen et al. demonstrated a size effect on the propensity to form macrocycle structures: the smaller b₂ and b₃ exclusively adopt oxazolone structures, whereas mid-sized fragments (b₄–b₇) exhibit a mixture of oxazolone and macrocycle structures; for the largest b fragment, b₈, only macrocycle structures were confirmed [18]. Similar trends were observed for b₂–b₄ for Leu-enkephalin [21], as well as b₅ from YAGFL-NH₂ [22]. Computational results by Bleiholder et al. confirmed that for permuted b₅ fragment ions, the macrocycle structures were energetically favored over the linear oxazolones [30].

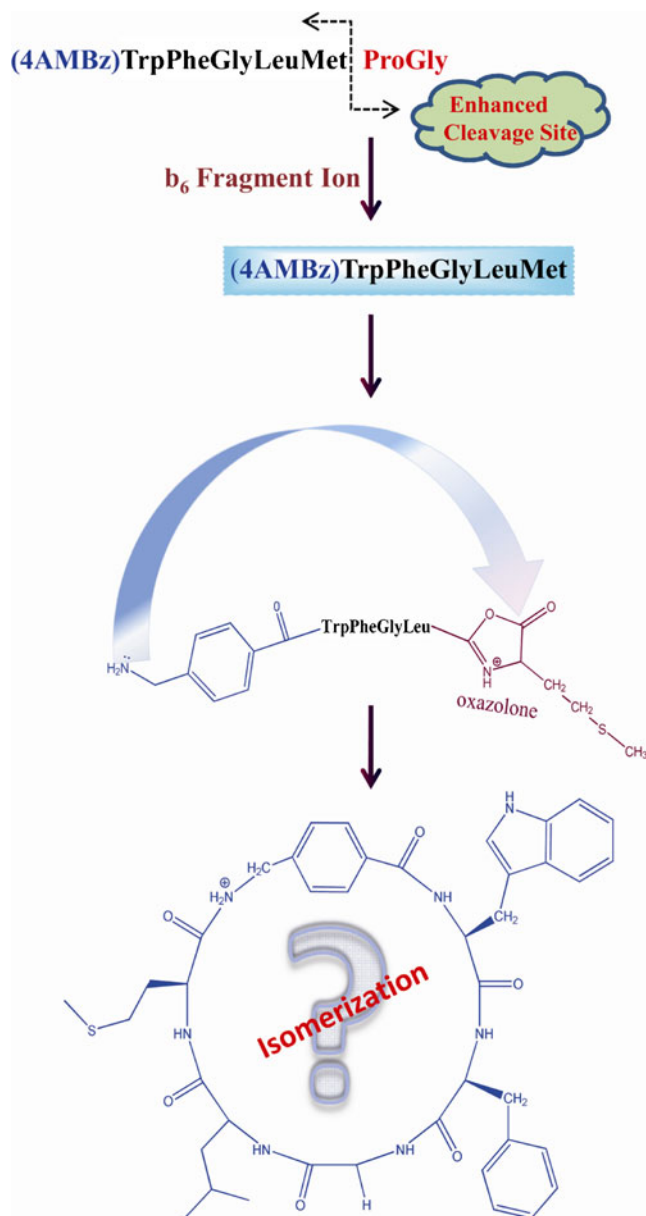
Analysis of tandem MS studies had shown significant formation of non-direct (i.e., permuted, scrambled) sequence ions for larger b_n ions [6, 11]. These findings are consistent with enhanced macrocycle formation for larger b_n fragments, as well as a higher proclivity for opening up at a different residue than where they were originally fused together. Nonetheless, it appears that some residues, such as arginine, can disrupt the scrambling chemistry, as shown by Van Stipdonk and coworkers [31]. This suggests that some amino acid residues may be capable of impeding macrocycle formation. From solution-phase cyclopeptide synthesis, it is well known that the conformational flexibility of cyclopeptides can be controlled by the introduction of rigid, non-natural amino acids in the ring. For instance, Kubik synthesized rigid cyclic hexapeptides composed of alternating L-glutamic acid and 3-aminobenzoic acid [32, 33]. Similarly, many cyclic peptides, such as gramicidin S, include proline residues. Work by van Maarseveen and co-workers further corroborates that through more aggressive chemistries such as Cu^I-catalyzed cycloaddition, the challenging synthesis of cyclo-[Pro-Val-Gly-ψ(triazole)-Tyr], a triazole analog of cyclo-[Pro-Val-Pro-Tyr], can readily be achieved in solution phase chemistry [34].

This study aims at determining how amino acid residues with limited torsional flexibility affect macrocycle formation in the b₆ fragment sequence motif QWFGLM, which has a very high propensity to form macrocycle structures [35]. The residues proline and 4-aminomethylbenzoic acid (**4AMBz**) were chosen here, in the expectation that their rigid structures may restrict “head-to-tail” cyclization from the N-terminus, as shown in Scheme 1.

Experimental

Sample Preparation

All peptides were synthesized with conventional Fmoc solid-phase synthesis methods using 9-fluorenylmethoxycarbonyl (Fmoc)-Gly loaded resin at the University of Florida [36, 37]. A CEM microwave discover system (Matthews, NC, USA) was utilized to synthesize 0.1 mmol scale of the corresponding peptides. Amino acid residues were purchased from Advanced Chem Tech (Louisville, KY, USA) and used as received without further purification. Briefly, upon completion of the synthesis, the peptide was cleaved from the resin using a 14 mL cocktail solution made up of 95% trifluoroacetic acid (TFA), 2.5% water, and 2.5% triisopropylsilane. Three rounds of purification and centrifugation were performed. The peptide was precipitated from the TFA solution with ice cold ether. After decanting the last amount of diethyl ether, a gentle stream of nitrogen gas was applied to the surface of the peptide to assist drying. All products had a brown color. High-performance liquid chromatography



Scheme 1. Schematic for formation of b₆ fragment, initially leading to oxazolone structure. Hypothesis of study: Limited torsional flexibility of e.g. 4AMBz residue restricts “head-to-tail” isomerization to macrocycle

(HPLC) and mass spectrometry was subsequently employed to assess product presence and purity. Typically, yields of greater than 90% were obtained.

The cyclic peptides were synthesized at the University of Amsterdam. First, the linear peptide QPFGLM was made with solid phase synthesis on a trityl resin. After cleavage and purification of the linear peptide, the peptides were dissolved in THF at concentrations of less than 10⁻³ mol/L, with 4.4 equivalent of *N,N*-diisopropylethylamine (DIPEA), 2.2 equivalent of 2-(1H-7-azabenzotriazol-1-yl)-1,1,3,3-tetramethyl uronium hexafluorophosphate methanaminium (HATU), and 3H-1,2,3-triazolo[4,5-*b*]pyridin-3-ol (HOAT)

were added into the solution. The reaction solution was kept at room temperature while stirring for 24 h. The aliquot from the reaction solution was characterized by LC/MS to ensure that the reaction went to completion. The THF was evaporated off from the reaction solution, and the remaining solid was then dissolved in ethyl acetate. 1 M KHSO₄ aqueous solution was added to dissolve the unreacted coupling reagents. The organic phase was collected and solid Na₂SO₄ was added to remove the remaining water. The organic phase was lyophilized to obtain solid products. The crude peptides were purified by reversed-phase HPLC (RF-HPLC) on a C18 column using a gradient of 0%–80% B (Buffer A: water/0.05%TFA; Buffer B: 90% acetonitrile/10% water/0.045% TFA) over 30 min.

Mass Spectrometry and Infrared Photodissociation Spectroscopy

IRMPD spectra of b ions were recorded using the free electron laser FELIX [38] located at the FOM institute for Plasma Physics Rijnhuizen. The ions were generated by electrospray ionization (ESI) in a home-built Fourier transform ion cyclotron resonance (FTICR) mass spectrometer described previously [39, 40]. Peptide solutions at 100 μM were prepared, composed of 50/50/2 (vol/vol/vol) water/methanol/formic acid. The fragment ions were generated by “nozzle-skimmer” dissociation in the ESI source. SWIFT excitation was used to isolate a specific b₆ fragment ion [41]. Following accumulation in the hexapole, the ions were transferred and guided by the octopole into the ICR cell. The mass-selected ion of interest was irradiated with 20–30 macropulses from the free electron laser FELIX. Each 5-μs macropulse is composed of a train of micropulses at a 1-GHz repetition rate. The energy per macropulse amounts to approximately 50 mJ, of which some 30 mJ finally makes it to the ion cloud in the ICR trap. The IRMPD spectrum was obtained by monitoring the IRMPD yield as a function of wavelength (1300–1975 cm⁻¹). The yield is given by the following equation: $\text{Yield} = -\ln[1 - (\sum \text{Int}_{\text{Photofragments}} / \sum \text{Int}_{\text{All Ions}})]$. The yield is further normalized linearly with the relative FELIX laser power at each wavelength step.

SORI CID Experiments

Complementary sustained off-resonance irradiation collision-induced dissociation (SORI CID) were carried out in a commercial FTICR mass spectrometer (4.7 T actively shielded APEX II, Bruker Daltonics, Billerica, MA, USA) at the University of Florida. The b CID product ions were generated by “nozzle-skimmer” dissociation in the ESI source. These b ions were then subjected to SORI CID in the ICR cell, using a frequency offset of -2.0 kHz (relative to the precursor ion’s cyclotron frequency) and a nitrogen gas pulse (<10⁻⁷ Torr).

Results and Discussion

The protonated precursor octapeptide **QWFGLMPG** was chosen to yield an abundant b_6 fragment, due to facile cleavage on the N-terminal side of proline. The IRMPD spectrum of this b_6 fragment is shown in Figure 1. Clearly, no bands are observed $>1770\text{ cm}^{-1}$, which indicates an absence of oxazolone structures. A comparison to the synthetically made cyclic peptide reference system, protonated cyclo(QWFGLM), which had been reported previously [18, 35], shows that both spectra are nearly identical. There are minor differences in the 1600 cm^{-1} region, which may suggest some differences in the conformational structures that are present. Nonetheless, the close similarity to the spectrum of the synthetic cyclic peptide provides compelling evidence that b_6 from QWFGLMPG exclusively adopts a macrocycle configuration, with no presence of oxazolone structures. This is in marked contrast to previous studies, where mid-sized b fragments were found to be comprised of a mixture of oxazolone and macrocycle structures [18, 21]. Sequence analogs of QWFGLMPG, incorporating proline and 4-aminomethylbenzoic acid (4AMBz) [42, 43], were synthesized to investigate their effect on macrocycle formation in the corresponding b fragment.

Proline

Due to its secondary amine structure, the proline residue adopts a fixed dihedral angle ($\sim 60^\circ$) in peptides on its N-terminal side [44]. In addition, proline is an endocyclic five-membered ring which introduces rigidity because no bond rotation is possible over the $C(\rightarrow)-N$ bond. Consequently, this rigidity may hamper closure due to unfavored preorganization of the N- and C-termini in the linear precursor. This strained geometry also rationalizes a weakening of the amide bond and, hence, enhanced fragmentation. A proline residue was substituted and inserted at position 2 in the sequence motif QWFGLM, to generate **QPFGLM** b_6 and **QPWFGLM** b_7 . In Figure 2, the experimental IRMPD spectra for the proline results are shown, spanning the mid-IR range ($1200\text{--}2000\text{ cm}^{-1}$). At the higher frequency portion of the spectrum, b_7 exhibits a broad and sizeable band position from $1770\text{--}1870\text{ cm}^{-1}$, consistent with an oxazolone C=O stretch. For b_6 , the presence of weaker oxazolone bands is manifested in a similar range (i.e., $1755\text{--}1870\text{ cm}^{-1}$). A comparison to the IR spectrum of the synthetically made cyclic structure analog, protonated cyclo-QPFGLM, confirms that b_6 parallels some spectroscopic features of b_7 more closely than those of its cyclic structural analogue, notably, at frequencies around 1700 cm^{-1} for the amide I band (i.e., backbone C=O stretch) and at $\sim 1450\text{ cm}^{-1}$. In addition, the absence of spectral features around 1600 cm^{-1} is similar for b_6 and b_7 fragment ions. The weaker oxazolone band for b_6 , in contrast to the more intense feature for b_7 , hints at the presence of additional structures for b_6 . Note that the IRMPD yields obtained for the b_6 and b_7 ions were 37% and 96%, respectively, under similar conditions.

The appearance of oxazolone structures for proline-containing peptides is consistent with restricted “head-to-tail” cyclization. Unfortunately, a detailed investigation of the effect of the position of proline on head-to-tail cyclization is complicated by prevalent cleavage on its N-terminal side. While proline in position 2 yields no abundant y_7 ions from QPFGLMPG (due to an inability to form b_1), proline substitutions in other position induce abundant cleavages, substantially reducing the abundance of the ion of interest here.

Aminomethylbenzoic Acid

Similarly to proline, incorporation of the non-natural amino acid **4AMBz** also leads to reduced torsional freedom in a peptide backbone. However, in contrast to proline, **4AMBz** does not give rise to redundant dissociation, such as (much) enhanced cleavage on its N-terminal side. Figure 3 shows the IRMPD spectra for the b_6 fragments with sequence motif QWFGLM, with different **4AMBz** substitutions. With the exception of **4AMBz** in the sixth position, all the corresponding b_6 ions were generated. Despite an intense precursor ion signal for QWFGL(4AMBz)PG, its b_6 fragment ion could not be produced. This is most likely attributed to the fact that **4AMBz** sterically hinders the nucleophilic attack from a backbone carbonyl, as depicted in Figure 4. The lack of a QWFGL(4AMBz) b_6 fragment is in accordance with the proposed mechanism that oxazolone structures are formed prior to isomerization to macrocycle structures [3]. In Figure 3, there is no evidence for oxazolone structures, with the exception of a weak feature between $1765\text{--}1860\text{ cm}^{-1}$ for **4AMBz** in position 5. In the corresponding oxazolone structure in Figure 5, the oxazolone ring and the benzene ring form a delocalized, resonantly-stabilized π -electron system. Such an extended

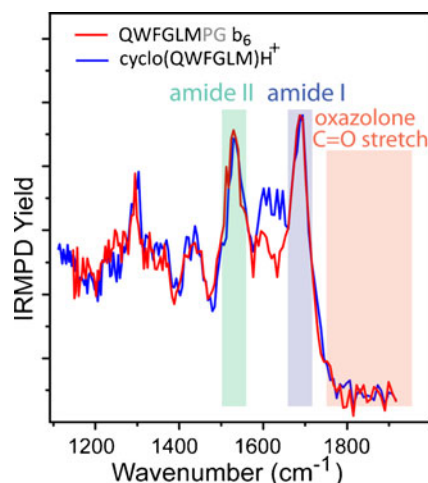


Figure 1. Overlay of IRMPD spectra of QWFGLMPG b_6 and protonated cyclo(QWFGLM). The chemically diagnostic regions are indicated by color-coding: oxazolone CO stretch (red), amide backbone CO stretch (blue), and amide backbone NH bending (green)

π -electron system is not possible for any of the other b fragments. It is hence likely that the small fraction of oxazolone structures for b_6 QWFG(4AMBz)M is due to a lowering in energy and hence stabilization of the oxazolone structure, due to this extended π -electron system, rather than an ability of 4AMBz in obstructing a head-to-tail cyclization. Similarly, Van Stipdonk and co-workers have noted an enhancement of b-type product ions when the aromatic amino residue 4AMBz was located in the penultimate position from the residue where amide cleavage takes place. This phenomenon is attributed to a highly conjugated and stable oxazolone structure stemming from the aromatic ring substituent 4AMBz [45, 46].

As a control experiment, a poor nucleophile analog of 4AMBz, 4-aminobenzoic acid (4Abz), was used to prevent head-to-tail macrocycle formation. In Figure 6, (4Abz)WFGML b_6 exhibits an intense oxazolone band from 1865–1970 cm^{-1} , in stark contrast to the absence of such a band for (4AMBz)WFGML b_6 . While the absence of oxazolone bands does not directly confirm the (exclusive) presence of macrocycle structures, the IRMPD spectra for 4AMBz inserted in positions 2–5 display similar amide I band positions compared with the protonated cyclic peptides, cyclo(QWFGML)H⁺, and cyclo(QPFGML)H⁺, even if the amide II (i.e., NH bending) positions are slightly red-shifted (10–15 cm^{-1}). The IRMPD spectrum for (4AMBz)WFGML b_6 differs from the other 4AMBz analogs, in that it displays an obvious splitting of the amide I stretching modes. The same effect is seen for (4Abz)WFGML b_6 , which suggests that this is related to the benzoic acid residue CO stretch.

Photofragmentation and SORI CID

In addition to the vibrational information from IRMPD spectra, the photofragmentation mass channels can offer insights whether the cyclic peptides in fact give rise to

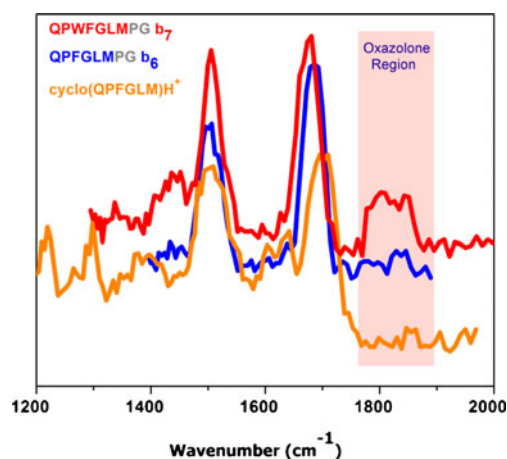


Figure 2. Overlay of IRMPD spectra of QPWFGMLPG b_7 , QPFGMLPG b_6 , and protonated cyclo(QPFGML). The chemically diagnostic oxazolone CO stretch region is highlighted in red

consecutive fragment ions with scrambled sequences. A comparison to SORI CID mass spectra can establish whether these fragmentation patterns are more general for low-energy activation methods. The SORI CID and IRMPD mass spectra for the control b_6 fragment from (4ABz)WFGMLPG are shown in Figure S1 (Supporting Information). IRMPD of (4ABz)WFGML b_6 exhibits a b ion series arising from cleavage propagating along the backbone. In the SORI CID experiment, many of the same fragments are confirmed (dashed lines), but additional fragments are observed when the precursor b_6 is depleted fully. In particular, the appearance of the internal fragment FGLM confirms that two backbone cleavages can take place under these conditions.

The SORI CID and IRMPD mass spectra for the b_6 CID products from (4AMBz)-substituted peptides are shown in Figure S2 (Supporting Information). The IRMPD photofragment channels are also summarized in Table S3 (Supporting Information). In the IRMPD results, despite considerable evidence for macrocycle formation in these b fragments, only one scrambled sequence ion could be identified. For (4AMBz)WFGML b_6 , the minor photofragment at m/z 552 could correspond to a scrambled (4AMBz)WFL a_4 (marked in red in Figure S2), requiring internal elimination of a glycine residue.

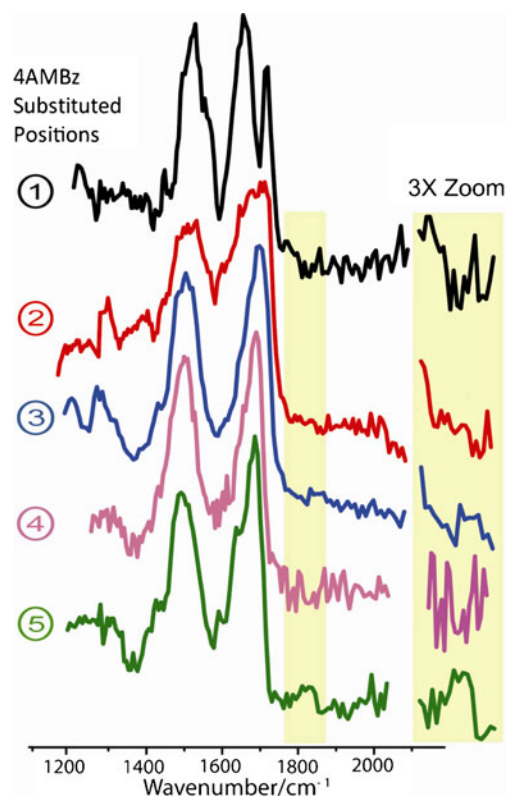


Figure 3. Overlay of IRMPD spectra for b_6 fragments with different 4AMBz substitutions in the sequence motif QWFGML. The inset shows a 3 \times vertical zoom of the 1780–1870 cm^{-1} region

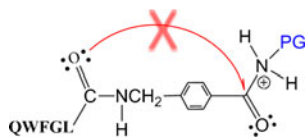


Figure 4. Reaction scheme showing impeded b_6 ion formation for QWFGL(4AMBz)PG due to bulky 4AMBz residue

Many additional fragments are seen in the corresponding SORI CID mass spectra. Some of these additional fragments are due to scrambled sequence ions (red), internal fragments (blue), or unknown rearrangements (*). For (4AMBz)WFGLM b_6 , the fragment at m/z 675 is assigned to an internal elimination of (Gly+H₂O); the fragment at m/z 621 is compatible with an internal elimination of phenylalanine. These sequential fragment ions likely arise from the formation of a macrocyclic structure that has reopened and undergone the loss of the aforementioned residues. Q(4AMBz)FGLM b_6 provides a lot of evidence for internal fragments, where abundant cleavage at the N-terminal side of 4AMBz occurs, as well as another backbone cleavage. On the other hand, for QW(4AMBz)GLM b_6 all consecutive fragments closely reflect the original sequence. For QWF(4AMBz)LM b_6 , few smaller fragments are observed. Finally, for QWFG(4AMBz)M b_6 abundant unassignable peaks are observed.

As a general observation, the consecutive fragmentation of these b_6 CID products exhibit extensive ammonia and water neutral loss products (e.g., b -NH₃ and b -H₂O), yet the corresponding b ions are often not observed. The high prevalence of b -NH₃ and b -H₂O fragments could be related to the presence of glutamine. It has been observed previously that when glutamine is on the N-terminus of a peptide chain, either water loss (-18 Da) or ammonia loss (-17 Da) can take place [47, 48]. In addition, Tabb et al. have noted in their statistical analysis of tandem mass spectra from tryptic peptides that the presence of glutamine leads to preferential ammonia loss [49].

Conclusions

In this study, we employed synthetic chemistry, IRMPD spectroscopy and SORI CID to carry out a systematic study on peptide b fragments with the sequence motif QWFGLM.

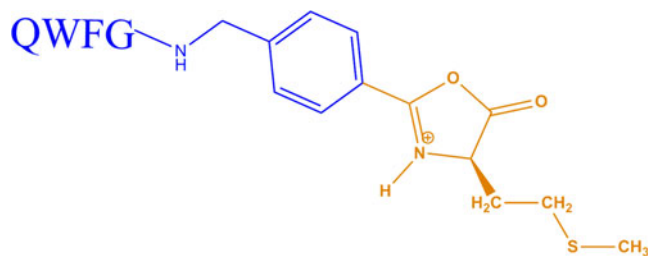


Figure 5. Resonantly-stabilized π -electron oxazolone ring structure for QWFG(AMBz)MPG b_6

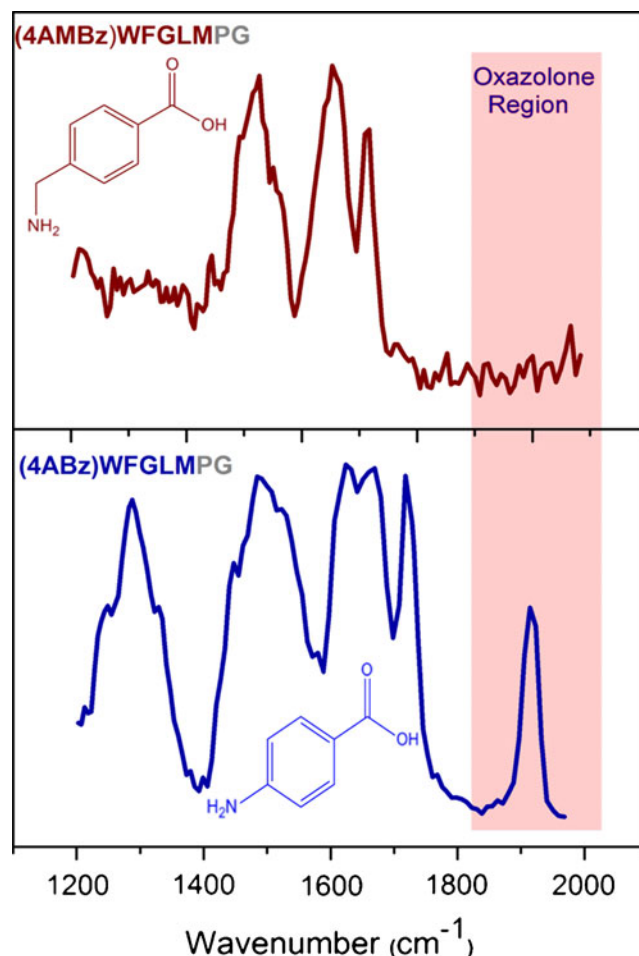


Figure 6. Comparison of IRMPD spectra of (4AMBz)WFGLMPG b_6 (top) and (4ABz)WFGLMPG b_6 (bottom). The chemically diagnostic oxazolone CO stretch region is highlighted in red. The chemical structures for 4-aminomethylbenzoic acid and 4-aminobenzoic acid are shown

The aim was to determine if amino acid residues with constrained torsional freedom affect macrocycle formation in the corresponding b fragment. The presence of proline in position 2 resulted in appearance of sizeable oxazolone bands for QPWFGLM b_7 and, to a lesser degree, in QPFGLM b_6 . This supports the hypothesis that constraining the flexibility of the backbone can suppress “head-to-tail” cyclization from the N-terminus. On the other hand, insertion of 4-aminomethylbenzoic acid (4AMBz) had little or no effect on macrocycle formation for b_6 , with the exception of a weak oxazolone band for QWFG(4AMBz)M b_6 , with 4AMBz in the fifth position. It is probable that this is mainly due to a lowering in energy of the oxazolone structure, as a result of a conjugated π -electron system between the benzene and oxazolone rings. An analysis of the photofragmentation channels provided scant evidence for scrambling phenomena, and rather abundant NH₃ and H₂O losses from b fragments are observed, in the absence of the corresponding b fragments. The SORI CID mass spectra show slightly more evidence for scrambling products, as

well as internal fragments, even if this is dependent on the sequence. The vibrational spectra demonstrate that the formation of macrocycle b structures can be surprisingly robust, and is difficult to disrupt, even using residues with limited torsional degrees of freedom. On the other hand, the prevalent formation of macrocycle structures does not necessarily result in scrambled sequence ions. This underlines the importance of the ring opening chemistry, as the barriers to ring opening are dependent on residue and ring configuration.

Acknowledgments

The skillful assistance of the FELIX staff, in particular Dr. Britta Redlich and Dr. Lex van der Meer, is gratefully acknowledged. Travel support to The Netherlands for M.T., X.C., and A.Y. was provided by the NSF-PIRE (OISE-0730072). N.P. thanks the University of Florida for start-up funds. This work is supported by the National Science Foundation under CHE-0845450. The American Society for Mass Spectrometry (2008 ASMS Research Award) is also acknowledged for their financial support on this project. Dr. David H. Powell is thanked for allowing access to his FT-ICR mass spectrometer. G.B. and J.O. were supported by the Nederlandse Organisatie voor Wetenschappelijk Onderzoek (Dutch National Science Foundation). Construction and shipping of the FTMS instrument was made possible through funding from the National High Field FT-ICR Facility (grant CHE-9909502) at the National High Magnetic Field Laboratory, Tallahassee, FL, on the initiative of Professor John R. Eyler and Professor Alan G. Marshall.

References

1. Yalcin, T., Khouw, C., Csizmadia, I.G., Peterson, M.R., Harrison, A.G.: Why are b ions stable species in peptide spectra? *J. Am. Soc. Mass Spectrom.* **6**, 1165–1174 (1995)
2. Yalcin, T., Csizmadia, I.G., Peterson, M.B., Harrison, A.G.: The structure and fragmentation of b_n ($n \geq 3$) ions in peptide spectra. *J. Am. Soc. Mass Spectrom.* **7**, 233–242 (1996)
3. Harrison, A.G., Young, A.B., Bleiholder, B., Suhai, S., Paizs, B.: Scrambling of sequence information in collision-induced dissociation of peptides. *J. Am. Chem. Soc.* **128**, 10364–10365 (2006)
4. Vachet, R.W., Bishop, B.M., Erickson, B.W., Glish, G.L.: Novel peptide dissociation: gas-phase intramolecular rearrangement of internal amino acid residues. *J. Am. Chem. Soc.* **119**, 5481–5488 (1997)
5. Harrison, A.G.: Peptide Sequence Scrambling Through Cyclization of b_5 Ions. *J. Am. Soc. Mass Spectrom.* **19**, 1776–1780 (2008)
6. Molesworth, S., Osburn, S., van Stipdonk, M.J.: Influence of size on apparent scrambling of sequence during CID of b-type ions. *J. Am. Soc. Mass Spectrom.* **20**, 2174–2181 (2009)
7. Harrison, A.: Cyclization of peptide b_9 ions. *J. Am. Soc. Mass Spectrom.* **20**, 2248–2253 (2009)
8. Boyd, R., Somogyi, A.: The mobile proton hypothesis in fragmentation of protonated peptides: A perspective. *J. Am. Soc. Mass Spectrom.* **21**, 1275–1278 (2010)
9. Saminathan, I.S., Wang, X.S., Guo, Y., Krakovska, O., Voisin, S., Hopkinson, A.C., Siu, K.W.M.: The extent and effects of peptide sequence scrambling via formation of macrocyclic b ions in model peptides. *J. Am. Soc. Mass Spectrom.* **21**, 2085–2094 (2010)
10. Goloborodko, A., Gorshkov, M., Good, D., Zubarev, R.: Sequence Scrambling in Shotgun Proteomics is Negligible. *J. Am. Soc. Mass Spectrom.* **22**, 1121–1124 (2011)
11. Yu, L., Tan, Y., Tsai, Y., Goodlett, D.R., Polfer, N.C.: On the Relevance of Peptide Sequence Permutations in Shotgun Proteomics Studies. *J. Proteome Res.* **10**, 2409–2416 (2011)
12. Campbell, S., Rodgers, M.T., Marzluff, E.M., Beauchamp, J.L.: Deuterium exchange reactions as probe of biomolecule structure. Fundamental studies of gas phase reactions of protonated glycine oligomers with D_2O , CD_3OD , CD_3CO_2D and ND_3 . *J. Am. Chem. Soc.* **117**, 12840–12854 (1995)
13. Eyler, J.R.: Infrared Multiple Photon Dissociation Spectroscopy of Ions in Penning Traps. *Mass Spectrom. Rev.* **28**, 448–467 (2009)
14. Polfer, N.C.: Infrared multiple photon dissociation spectroscopy of trapped ions. *Chem. Soc. Rev.* **40**, 2211–2221 (2011)
15. Clemmer, D.E., Jarrold, M.F.: Ion mobility measurements and their applications to clusters and biomolecules. *J. Mass Spectrom.* **32**, 577–592 (1997)
16. Polfer, N.C., Bohrer, B.C., Plasencia, M.D., Paizs, B., Clemmer, D.E.: On the dynamics of fragment isomerization in collision-induced dissociation of peptides. *J. Phys. Chem. A* **112**, 1286–1293 (2008)
17. Garcia, I., Giles, K., Bateman, R.H., Gaskell, S.J.: Evidence for structural variants of a- and b-type peptide fragment ions using combined ion mobility/mass spectrometry. *J. Am. Soc. Mass Spectrom.* **19**, 609–613 (2008)
18. Chen, X., Yu, L., Steill, J.D., Oomens, J., Polfer, N.C.: Effect of peptide fragment size on the propensity of cyclization in collision-induced dissociation: oligoglycine b_2 - b_8 . *J. Am. Chem. Soc.* **131**, 18272–18282 (2009)
19. Perkins, B., Chamot-Rooke, J., Yoon, S., Gucinski, A., Somogyi, A., Wysocki, V.H.: Evidence of diketopiperazine and oxazolone structures for HA b_2^+ ion. *J. Am. Chem. Soc.* **131**, 17528–17529 (2009)
20. Fattahi, A., Zekavat, B., Solouki, T.: H/D exchange kinetics: Experimental evidence for formation of different ion conformers/isomers during the gas-phase sequencing. *J. Am. Soc. Mass Spectrom.* **21**, 358–369 (2009)
21. Chen, X., Steill, J.D., Oomens, J., Polfer, N.C.: Oxazolone versus macrocycle structures for Leu-enkephalin b_2 - b_4 : Insights from infrared multiple-photon dissociation spectroscopy and gas-phase hydrogen/deuterium exchange. *J. Am. Soc. Mass Spectrom.* **21**, 1313–1321 (2010)
22. Gucinski, A., Somogyi, Á., Chamot-Rooke, J., Wysocki, V.: Separation and identification of structural isomers by quadrupole collision-induced dissociation-hydrogen/deuterium exchange-infrared multiphoton dissociation (QCID-HDX-IRMPD). *J. Am. Soc. Mass Spectrom.* **21**, 1329–1338 (2010)
23. Li, X., Huang, Y., O'Connor, P., Lin, C.: Structural heterogeneity of doubly-charged peptide b-ions. *J. Am. Soc. Mass Spectrom.* **22**, 245–254 (2011)
24. Polfer, N.C., Oomens, J., Suhai, S., Paizs, B.: Spectroscopic and theoretical evidence for oxazolone ring formation in collision-induced dissociation of peptides. *J. Am. Chem. Soc.* **127**, 17154–17155 (2005)
25. Polfer, N.C., Oomens, J., Suhai, S., Paizs, B.: Infrared spectroscopy and theoretical studies on gas-phase protonated leu-enkephalin and its fragments: Direct evidence for the mobile proton. *J. Am. Chem. Soc.* **129**, 5887–5897 (2007)
26. Yoon, S., Chamot-Rooke, J., Perkins, B., Hilderbrand, A.E., Poutsma, J., Wysocki, V.H.: IRMPD spectroscopy shows that AGG forms an oxazolone b ion. *J. Am. Chem. Soc.* **130**, 17644–17645 (2008)
27. Oomens, J., Young, S., Molesworth, S., van Stipdonk, M.J.: Spectroscopic evidence for an oxazolone structure of the b_2 fragment ion from protonated tri-alanine. *J. Am. Soc. Mass Spectrom.* **20**, 334–339 (2009)
28. Wang, D., Gulyuz, K., Stedwell, C., Polfer, N.: Diagnostic NH and OH Vibrations for oxazolone and diketopiperazine structures: b_2 from protonated triglycine. *J. Am. Soc. Mass Spectrom.* **22**, 1197–1203 (2011)
29. Bythell, B., Erlekam, U., Paizs, B., Maitre, P.: Infrared spectroscopy of fragments from doubly protonated tryptic peptides. *Chem. Phys. Chem.* **10**, 883–885 (2009)
30. Bleiholder, C., Osburn, S., Williams, T., Suhai, S., van Stipdonk, M.J., Harrison, A.G., Paizs, B.: Sequence-scrambling fragmentation pathways of protonated peptides. *J. Am. Chem. Soc.* **130**, 17774–17789 (2008)
31. Molesworth, S., Van Stipdonk, M.: Apparent inhibition by arginine of macrocyclic ion formation from singly charged protonated peptides. *J. Am. Soc. Mass Spectrom.* **21**, 1322–1328 (2010)
32. Kubik, S.: Large increase in cation binding affinity of artificial cyclopeptide receptors by an allosteric effect. *J. Am. Chem. Soc.* **121**, 5846–5855 (1999)

33. Pohl, S., Goddard, R., Kubik, S.: A new cyclic tetrapeptide composed of alternating l-proline and 3-aminobenzoic acid subunits. *Tetrahedron Lett.* **42**, 7555–7558 (2001)
34. Springer, J., de Cuba, K.R., Calvet-Vitale, S., Geenevasen, J.A.J., Hermkens, P.H.H., Hiemstra, H., van Maarseveen, J.H.: Backbone amide linker strategy for the synthesis of 1,4-triazole-containing cyclic tetra- and pentapeptides. *Eur. J. Org. Chem.* **2008**, 2592–2600 (2008)
35. Chen, X., Tirado, M., Steill, J.D., Oomens, J., Polfer, N.C.: Cyclic peptide as reference system for b ion structural analysis in the gas phase. *J. Mass Spectrom.* **46**, 1011–1015 (2011)
36. Chan, W.W.P. (ed.): Fmoc Solid Phase Peptide Synthesis—A Practical Approach. Oxford University Press Inc, New York (2000)
37. Kates, S.A., Albericio, F. (eds.): Solid-Phase Synthesis A Practical Guide. Marcel Dekker, Inc, New York (2000)
38. Oepts, D., van der Meer, A.F.G., van Amersfoort, P.W.: The free-electron-laser user facility FELIX. *Infrared Phys. Technol.* **36**, 297–308 (1995)
39. Valle, J.J., Eyler, J.R., Oomens, J., Moore, D.T., van der Meer, A.F.G., von Helden, G., Meijer, G., Hendrickson, C.L., Marshall, A.G., Blakney, G.T.: A free electron-Fourier transform ion cyclotron resonance mass spectrometry facility for obtaining infrared multiphoton dissociation spectra of gaseous ions. *Rev. Sci. Instrum.* **76**, 23103 (2005)
40. Polfer, N.C., Oomens, J., Moore, D.T., von Helden, G., Meijer, G., Dunbar, R.C.: Infrared spectroscopy of phenylalanine Ag(I) and Zn(II) complexes in the gas phase. *J. Am. Chem. Soc.* **128**, 517–525 (2006)
41. Wang, T.C.L., Ricca, T.L., Marshall, A.G.: Extension of dynamic range in Fourier transform ion cyclotron resonance mass spectrometry via stored waveform inverse Fourier transform excitation. *Anal. Chem.* **58**, 2935–2938 (1986)
42. Anbalagan, V., Silva, A.T.M., Rajagopalachary, S., Bulleigh, K., Talaty, E.R., Van Stipdonk, M.J.: Influence of “Alternative” C-terminal amino acids on the formation of [b3+17+Cat]⁺ products from metal cationized synthetic tetrapeptides. *J. Am. Soc. Mass Spectrom.* **39**, 495–504 (2004)
43. Cooper, T.J., Talaty, E.R., Van Stipdonk, M.J.: Novel fragmentation pathway for CID of (b(n)-1+Cat)⁺ ions from model, metal cationized peptides. *J. Am. Soc. Mass Spectrom.* **16**, 1305–1310 (2005)
44. Chatterjee, S., Roy, R.S., Balaram, P.: Expanding the polypeptide backbone: hydrogen-bonded conformations in hybrid polypeptides containing the higher homologues of α -amino acids. *J. R. Soc. Interface* **4**, 587–606 (2007)
45. Talaty, E.R., Cooper, T.J., Osburn, S., Van Stipdonk, M.J.: Collision-induced dissociation of protonated tetrapeptides containing β -alanine, γ -aminobutyric acid, ϵ -aminocaproic acid or 4-aminomethylbenzoic acid residues. *Rapid Commun. Mass Spectrom.* **20**, 3443–3455 (2006)
46. Osburn, S., Ochola, S., Talaty, E., Van Stipdonk, M.: Influence of a 4-aminomethylbenzoic acid residue on competitive fragmentation pathways during collision-induced dissociation of metal-cationized peptides. *Rapid Commun. Mass Spectrom.* **21**, 3409–3419 (2007)
47. Neta, P., Pu, Q.-L., Kilpatrick, L., Yang, X., Stein, S.E.: Dehydration versus deamination of N-terminal glutamine in collision-induced dissociation of protonated peptides. *J. Am. Soc. Mass Spectrom.* **18**, 27–36 (2007)
48. Godugu, B., Neta, P., Simón-Manso, Y., Stein, S.E.: Effect of N-terminal glutamic acid and glutamine on fragmentation of peptide ions. *J. Am. Soc. Mass Spectrom.* **21**, 1169–1176 (2010)
49. Tabb, D.L., Smith, L.L., Brechi, L.A., Wysocki, V.H., Lin, D., Yates III, J.R.: Statistical characterization of ion trap tandem mass spectra from doubly charged tryptic peptides. *Anal. Chem.* **75**, 1155–1163 (2003)